Available online at www.sciencedirect.com
ScienceDirect
Composites: Part A 38 (2007) 252–264
composites
Part A: applied science and manufacturing
www.elsevier.com/locate/compositesa

Effect of soy spent flakes and carbon black co-filler in rubber composites

L. Jong *

United States Department of Agriculture[1], National Center for Agricultural Utilization Research, Agricultural Research Service, 1815 North University Street, Peoria, IL 61604, USA

Received 13 December 2005; received in revised form 3 May 2006; accepted 4 May 2006

Abstract

The rubber composites that are reinforced by a mixture of soy spent flakes (SSF) and carbon black (CB) are investigated in terms of their viscoelastic properties. Soy spent flakes is a plentiful renewable material from the waste stream of commercial soy protein extraction. SSF contains mostly soy carbohydrate and dry SSF increases rubber modulus significantly. The aqueous dispersions of SSF and CB were first mixed and then blended with styrene–butadiene latex to form rubber composites by freeze-drying and compression molding method. The mixtures of SSF and CB at three different ratios are investigated as co-fillers. A 30% co-filler reinforced composite exhibits about 100 times increase in the shear elastic modulus compared with unfilled SB rubber, showing a significant reinforcement effect by the co-filler. Compared with the SSF composites, the recovery behaviors of the co-filler composites after the eight consecutive deformation cycles of dynamic strain are improved and are similar to that of the CB composites. The comparison of viscoelastic properties of the composites prepared by freeze-drying and casting methods indicates the composites prepared by freeze-drying method have a lower elastic modulus, but have a better recovery behavior due to its polymer mediated filler network structure. The co-filler composites with 50–75% substitution of CB by SSF have a greater elastic modulus than the CB reinforced composites.
Published by Elsevier Ltd.

Keywords: A. Particle-reinforcement; B. Rheological properties; B. Thermomechanical; Soy spent flakes

1. Introduction

For practical applications, rubber material is usually reinforced with fillers. Carbon black is the most often used filler. Carbon black is mainly derived from aromatic oil in petroleum or from natural gas. Substitution of carbon black with renewable filler has been investigated in recent years. Recent studies reported the modulus enhancement of rubbers by natural materials, for example, oil palm wood [1], crab shell chitin [2], and bamboo fiber [3]. From the perspective of renewable materials and environmental reasons, soy protein and other soybean products have been investigated as a component in plastic and adhesive applications [4–8], but have been rarely investigated as a reinforcement component in elastomers. Attempts to use protein in rubber latex can be traced back to the 1930s. A few patents [9–11] had claimed the use of protein in rubber composites. For example, Lehmann and co-workers had demonstrated the use of casein (milk protein) in natural rubber latex to achieve approximately a fourfold increase in the modulus [11]. Protein as an additive in rubber materials has also been claimed to improve the anti-skid resistance of winter tread tires [12–14]. In rubber reinforcement, factors such as aggregate structure, effective filler volume fraction, filler–rubber interaction and elastic modulus of filler clusters have important impact on the modulus of rubber composites [15]. Mechanically, the

[1] Names are necessary to factually report on available data; however, the USDA neither guarantees nor warrants the standard of the product, and the use of the name by USDA implies no approval of the product to the exclusion of others that may also be suitable.

* Tel.: +1 309 681 6240; fax: +1 309 681 6685.
E-mail address: jongl@ncaur.usda.gov

1359-835X/$ - see front matter Published by Elsevier Ltd.
doi:10.1016/j.compositesa.2006.05.003

elastic modulus of base rubber is not significant when compared with the modulus of filler network in highly filled elastomeric composites [16]. For practical applications, the issue of moisture sensitivity in some applications is always associated with natural materials, but it can be improved through product formulation, processing method, or selective applications. For example, it may be used as an ingredient in multilayered structures, in coated objects, in high temperature applications or in a rubber part used in greasy/oily environments, where the moisture effect is minimal.

The rubber matrix used in this study is a styrene–butadiene (SB) rubber with small amount of carboxylic acid containing monomer units. The carboxylated SB forms a crosslinked rubber by the aggregation of ionic functional groups without the complication of covalent reactions. Carboxylated SB rubber is classified as an ion-containing polymer. Its viscoelastic properties are affected by molecular weight, degree of crosslinking, glass transition temperature (T_g), copolymer composition, the number of ionic functional groups, the size of ionic aggregation, the degree of neutralization, and the size of the neutralizing ions [17,18]. Previous studies also have shown honeycomb-like structures in the film of carboxylated latexes due to a higher concentration of carboxylic acid groups on the particle surface [19]. Previous studies have indicated the importance of interaction between filler and matrix [16]. Soy protein contains a significant amount of carboxylic acid and substituted amine group [20]. Soy carbohydrate can also interact with carboxylic functional groups in SB matrix through hydrogen bonding and ionic interaction. Structurally, Soy protein is a globular protein and its aggregate is similar to colloidal aggregates, but soy carbohydrate is non-globular and film-like materials [21]. Although ionic interactions can occur between these soy products and the carboxylated SB, the condensation reactions do not occur under the alkali condition between the carboxyl groups of SB and the major functional groups such as hydroxyl, carboxyl, thiol, amine, and amide groups in SSF.

Soy spent flakes (SSF) used in this study is mostly a soy carbohydrate fraction in soybean. Soybean can be processed into soybean oil and defatted soy flour. SSF is mostly an insoluble carbohydrate after most of soy protein and soy whey, a soluble carbohydrate, are removed from defatted soy flour. SSF is a by-product or residue in the commercial extraction process of soy protein isolate. It is an abundant and inexpensive renewable material, but it has little commercial value at this time. The composition of SSF is approximately 12% cellulose, 17% pectin, 14% protein, and 53% insoluble polysaccharide [22]. SSF is desirable to be used in the as-is form from the commercial process without further separation so that its cost is comparable to inorganic fillers. SSF has the lowest cost among soy products such as defatted soy flour, soy protein concentrate, and soy proteins isolate (SPI), whereas SPI has the highest cost. Dry SSF is a rigid material and has a shear elastic modulus of ~4 GPa (Fig. 1) under ambient conditions. Because the high rigidity of a reinforcement phase is one of the requirements in rubber reinforcement, dry SSF is therefore a possible candidate for this application. However, previous studies indicate SSF reinforced rubber composites have less than desired modulus recovery after the consecutive deformation cycles [21]. In this study, the objective is to explore the co-filler effect by using a mixture of SSF and CB as reinforcement fillers. Another objective is to obtain more insight on the reinforcement mechanism by comparing different preparation methods—casting vs. freeze-drying.

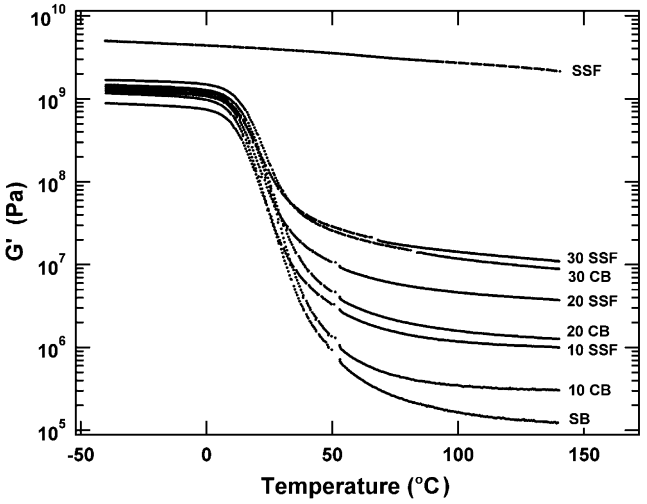

Fig. 1. Elastic moduli of SSF and CB composites. The weight fraction of filler is indicated at the end of each curve.

2. Experimental

2.1. Materials

In this study, SSF was obtained from defatted soy flour (DSF), a spray dried powder (Nutrisoy 7B) from Archer Daniels Midland Company, Decatur, IL. SSF can also be obtained commercially. A conventional process was used to separate SSF by removing alkali soluble protein and whey. ~300 g of DSF was first dispersed in water at ~13% concentration, pH ~ 10, and 45 °C for 1 h, and followed by centrifuged at 3000 rpm for 10 min at 15 °C to separate insoluble SSF. The SSF obtained was washed with ~900 g of water twice and centrifuged to obtain the final product. The yield of SSF based on dry DSF is ~23%, similar to that by industrial process. The composition of SSF is also similar to that by industrial process mentioned in the introduction. The resulting SSF paste with a solid content of 7.5% was used to prepare rubber composites. Sodium hydroxide, used to adjust pH, was ACS grade. The SPI used in this research is a slightly enzyme hydrolyzed soy protein isolate (PRO-FAM 781, Archer Daniels Midland Company, Decatur, IL). It contains more than 90% protein, ~6% ash and ~4% fat. Aqueous dispersion of carbon

black N-339 (Sid Richardson Carbon Co.) was prepared by dispersing ~100 g of carbon black (CB) in water with the aid of a surfactant, sodium lignosulfonate (Vanisperse CB, Lignotech USA, Rothschild, WI). The weight fraction of the surfactant based on carbon black is 3%. The dispersion was homogenized at 10^4 rpm for 1 h. The resulting CB dispersion has a solid content of 12.7%. The carboxylated styrene–butadiene (SB) latex used as rubber matrix is a random copolymer of styrene, butadiene, and small amount of carboxylic acid containing monomers [20] (CP 620NA, Dow Chemical Company, Midland, MI.). The glass transition temperature of carboxylated SB Latex is ~10 °C determined by DSC. Styrene/butadiene ratio estimated from the glass transition temperatures of a series of commercially available carboxylated styrene butadiene was about 65/35. The dried latex is not known to be soluble in any solvent or a combination of solvents due to ionic bonding. The latex received had ~50% solids and a pH ~ 6. The volume weighted mean particle size of latex was ~0.18 μm.

2.2. Preparation of elastomer composites

In this study, freeze-drying and compression molding method is preferred because there is a density difference between SSF and CB. Casting method may produce a less homogeneous sample. SSF in a paste form from the centrifuge step mentioned above was blended homogeneously with carbon black dispersion at three different dry weight ratios (1:3, 1:1 and 3:1). The SB latex, already adjusted to pH 9, was then added to the filler mixture and mixed homogeneously to form composites with three different filler contents (10 wt%, 20 wt%, and 30 wt%). The homogeneous composite mixtures were then quickly frozen in a rotating shell freezer at about −40 °C and followed by freeze-drying in a freeze-dryer (LABCONCO, Kansas City, MO). The moisture content of dried composite crumb is less than 2%. The freeze-dried crumb was compression molded in a plunge type mold at 69 MPa and 140 °C for 2.5 h. After compression molding, the samples were relaxed and further annealed at 95 °C, 110 °C, and 140 °C for 24 h, respectively. The torsion bars of 100% carboxylated SB rubber and SSF were prepared by the same process as that of the co-filler composites. The dried samples had moisture contents less than 0.8% as measured by halogen moisture analyzer (Mettler Toledo HR73) at 105 °C for 60 min. For comparison, SSF and CB composites were prepared by using the same procedure as that of co-filler composites. The densities of SSF, CB, and SB were measured by using a density bottle with a low viscosity poly(dimethylsiloxane) as the immersion liquid.

2.3. Dynamic mechanical measurements

A Rheometric ARES-LSM rheometer (TA Instruments, Piscataway, NJ) was used in the dynamic mechanical measurements. Temperature ramp experiments were conducted using torsion rectangular geometry with a heating rate of 1 °C/min in a temperature range from −40 °C to 140 °C. The soak time at each temperature after ramp was 15 s and the measurement duration at each temperature was 30 s. When using torsion rectangular geometry, torsional bars with dimensions of approximately $40 \times 12.5 \times 3$ mm were mounted between a pair of torsion rectangular fixtures and the dynamic mechanical measurements were conducted at a frequency of 0.16 Hz (1 rad/s) and a strain of 0.05%.

For the strain sweep experiments, the oscillatory storage and loss moduli, $G'(\omega)$ and $G''(\omega)$, were measured using a torsional rectangular geometry. The shear strain-controlled rheometer is capable of measuring the oscillatory strain down to 3×10^{-5} % strain (TA Instruments, Piscataway, NJ). The rheometer was calibrated in terms of torque, normal force, phase angle, and strain using the instrument procedure. A rectangular sample with dimension of approximately $12.5 \times 20 \times 4$ mm was inserted between the top and bottom grips. The gap between the fixtures was ~7 mm in order to achieve a strain of ~14%. A sample length shorter than 5 mm is not desirable because of the shape change from the clamping at both ends of the sample. The frequency used in the measurements was 1 Hz. The oscillatory storage and loss moduli were measured over a strain range of approximately 0.001–14%. The actual strain sweep range was limited by sample geometry and motor compliance at large strain, and transducer sensitivity at small strain. The data that was out of the transducer range was rejected. Although harmonics in the displacement signal may be expected in non-linear material, a previous study [23] indicated that the harmonics are not significant if the shearing does not exceed 100%. Each sample was conditioned at 140 °C for 30 min and then subjected to 8 cycles of dynamic strain sweep in order to study the stress softening effect. The delay between strain cycles is 100 s. For clarity, only data from the first, fourth, and eighth cycle are presented in the figures. To measure the recovery curves, the samples after subjected to eight strain cycles were allowed to recover at 140 °C for 24 h before they were subjected to one cycle of strain sweep.

3. Results and discussion

3.1. Comparison of casting and freeze-drying methods

The rubber composites prepared by casting and freeze-drying method exhibit different mechanical properties due to their different filler network structures. The comparison of these reinforcement structures is therefore instructive to understand the reinforcement mechanism of rubber composites. In this study, the range of filler fractions in the composites is above the percolation threshold, which means the fillers can form a network due to the presence of a sufficient number of filler aggregates in the rubber matrix. Fig. 1 shows the dynamic shear elastic moduli of SSF and CB composites prepared by freeze-drying method.

The composite filled with 30% SSF exhibits about 100 times increase in the G' compared with the unfilled SB rubber. In the 10% and 20% filled composites, SSF composites have a significantly greater G' than CB composites within the rubber plateau region. In the 30% filled composites, G' of SSF composite is slightly higher than that of CB composite. The comparison is based on the weight fraction of filler, which is relevant to the economic value of the filler. It should be noted that SSF has a density of 1.50 g/cm^3 and CB has a density of 1.73 g/cm^3. Therefore, SSF has a greater volume fraction than CB at the same weight fraction and the reinforcement effect is proportional to the volume fraction instead of weight fraction. However, other factors such as aggregate size of filler, filler–filler interaction, and filler–rubber interactions also contribute to the observed modulus behavior. The number average size of wet SSF is ~10 μm and the dry size is ~7 μm by correcting the swelling effect in water. The number average size of CB aggregates is ~0.3 μm [17,24]. The effects of aggregate size and filler–filler interaction have been reported previously [17,24].

Fig. 2 shows the comparison of SSF and CB composites, and the comparison of these composites prepared by casting and freeze-drying methods. The mechanical properties of composites prepared by the casting method have been reported previously [17,24]. Generally, the SSF composites have a greater G' than that of the CB composites and the composites prepared by the casting method have a greater G' than that prepared by the freeze-drying method. In the previous study, the greater G' of the SSF composites is attributed to a greater filler network strength through filler–filler interactions compared with the CB composites [17]. The greater G' in composites prepared by casting method, vs. freeze-drying method, can also be explained by the strength of filler network. The casting method is a slow process which allows the fillers to associate with each other as water evaporates. The freeze-drying method on the other hand produces a homogeneous mixture of filler and rubber particles, where filler aggregates are surrounded by the rubber particles because the filler has a smaller volume fraction in the mixture. Upon compression molding of freeze-dried crumbs, the filler network structure has increasing presence of a polymer layer sandwiched between filler aggregates compared with the filler network structure produced by the casting method. With the same filler, filler aggregate size, and filler volume fraction, a filler network with increasing presence of a polymer layer between filler aggregates is softer than a filler network without polymer mediation. Therefore, polymer mediation model [25] is adequate in explaining these differences. Another variable is that the composites prepared by freeze-drying method may have a thicker polymer layer between filler aggregates and thus have a softer filler network structure because the rigid immobilized polymer layer possibly only extends a few nanometers [26] outward from the filler surface.

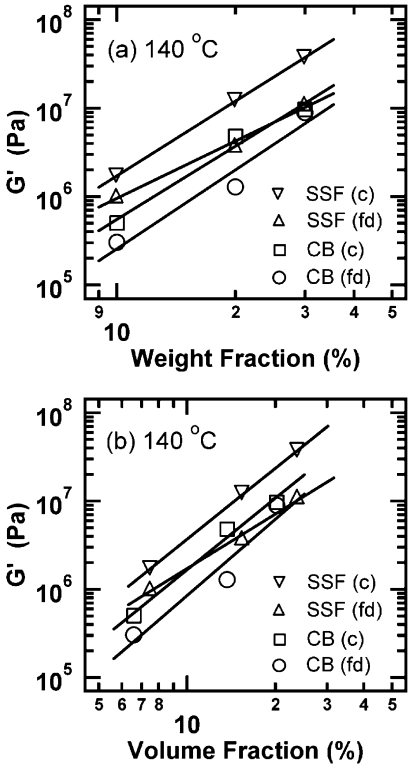

Fig. 2. Elastic moduli of SSF and CB composites at small strain region plotted against weight and volume fractions. c = casting and fd = freeze-drying. The measurements were conducted at 0.16 Hz and 140 °C.

3.2. Filler–rubber interactions in SSF and CB composites

The information of filler–rubber interaction can be obtained from the shifting of loss maximums of these

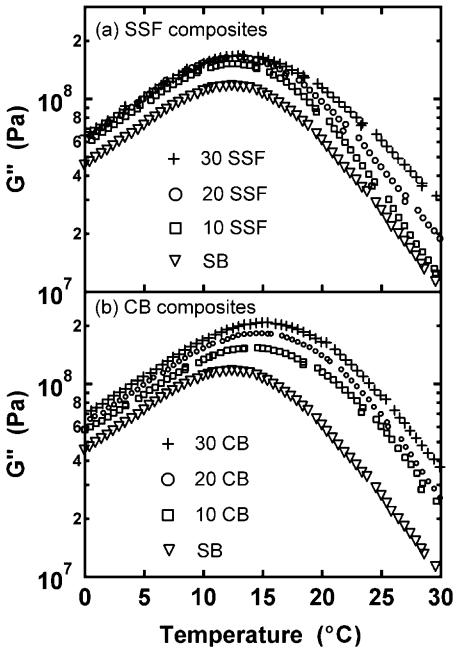

Fig. 3. Loss moduli of SSF and CB composites prepared by freeze-drying method.

composites in Fig. 3, which shows the G'' of SSF and CB composites in the glass transition region. The loss maximums represent the temperature at which the energy loss as heat from the composite structure reaches its maximum and is corresponding to the glass transition temperature. There is no significant shifting in the loss maximum of the SSF composites as SSF fraction in the composites is increased. The shifting of the loss maximum to a higher temperature in the CB composites is however observable as the CB concentration is increased. This is an indication that there is a greater extent of filler–rubber interaction in the CB composites because the fraction of filler-immobilized polymer has increased and resulted in a few degrees increase in the average glass transition temperature of SB rubber matrix. Whether the effect is due to a stronger filler–rubber interaction is not known, but the greater filler surface area from the smaller CB aggregates certainly contributes to such effect. A similar trend was observed on the same composites prepared by the casting method [24]. The same trend was also observed in $\tan\delta$ maximums in Fig. 4(a), it shows an insignificant shifting of $\tan\delta$ maximum as the SSF content is increased, similar to the trend of G'' maximum. A significant shifting of $\tan\delta$ maximum was observed in the CB composites (Fig. 4(b)) and the shifting is towards a lower temperature as the CB content is increased. This trend was also observed in soy protein [27], silica [28], and crosslinked polymer fillers [26]. The shifting direction of $\tan\delta$ maximum cannot be interpreted directly with a simple model of filler-immobilized polymer structure because it is a ratio of G''/G'. However, a tendency to shift along the temperature axis is similar to that of G'' maximum although in the opposite direction. For damping behaviors shown in Fig. 4, the magnitude of $\tan\delta$ is decreased as the filler content is increased. This behavior is typical in filled rubber composites. In the rubbery region of 120–140 °C, the damping of SSF composites is similar to that of CB composites.

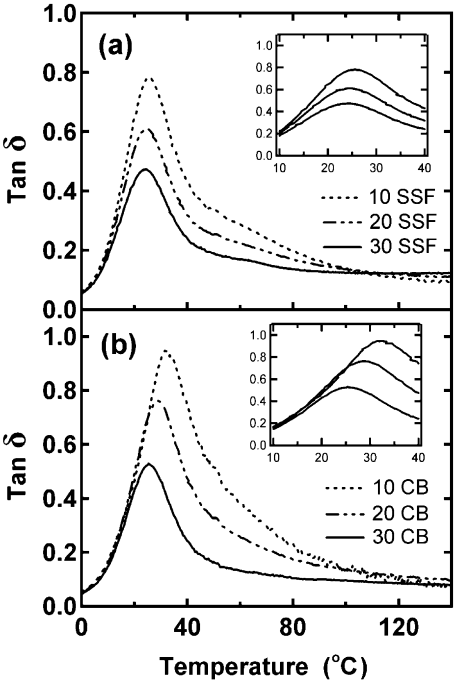

Fig. 4. Loss tangent of: (a) SSF and (b) CB composites prepared by freeze-drying method.

3.3. Non-linear viscoelastic properties of SSF and CB composites

Non-linear viscoelastic behaviors of these composites were investigated by using a series of strain cycles. Fig. 5 shows the effect of oscillatory strain cycles on the modulus of the composites. The effect is called stress softening, which occurs in most filled elastomers. It is defined as the stress needed to deform the filled rubber at a given elongation is reduced during the second cycle of deformation. The effect is also called Mullin effect for his extensive studies [29,30] on this phenomenon. The stress softening effect is generally considered to be caused by filler related structures and therefore can yield some insight into the filler structures [21]. For 30% SSF composite (Fig. 5(a)) prepared by freeze-drying method, G' of the eighth strain cycle in the small strain region is reduced to ~80% of its value in the first strain cycle. For the same composite prepared by the casting method, the retention of G' in the eighth cycle is ~60% of that in the first cycle. This indicates the composites prepared by freeze-drying method have a greater ability to instantly recover their filler network related structures. The recovery curves in Fig. 5 also indicate the same trend. This behavior is consistent with the previously mentioned polymer mediated filler network structure. G'' curves in Fig. 5 also demonstrate the structure difference in the composites prepared by these two different methods. Fig. 5(a) shows a loss maximum occurs at 7% strain and a secondary peak at 0.3% strain for the SSF composite prepared by freeze-drying method, while a G'' maximum occurs at 0.07% strain and a secondary peak at 3% strain for the SSF composite prepared by casting method. This indicates filler related network structure of the composite prepared by freeze-drying method is more elastic because its G'' maximum, from the breaking down structure responsible for heat dissipation process, occurs at a larger strain when compared with the structure of the composite prepared by the casting method. The magnitude of damping ($\tan\delta$) within the same range of strain (Fig. 5(a) and (b)) is similar in the composites prepared by these two different methods.

For 30% CB composites prepared by these two different methods, a similar trend as that in SSF composites was observed. Fig. 6(a) shows G' of the CB composite has a 100% modulus recovery after 8 cycles of strain sweep and G' of the CB composite prepared by casting method has only ~70% of modulus recovery when compared with the G' of the first cycle (Fig. 6(b)). Filler related network structure responsible for heat dissipation, shown as G'' maximum, also occurs at a larger strain for the CB composite prepared by the freeze-drying method, while that of the

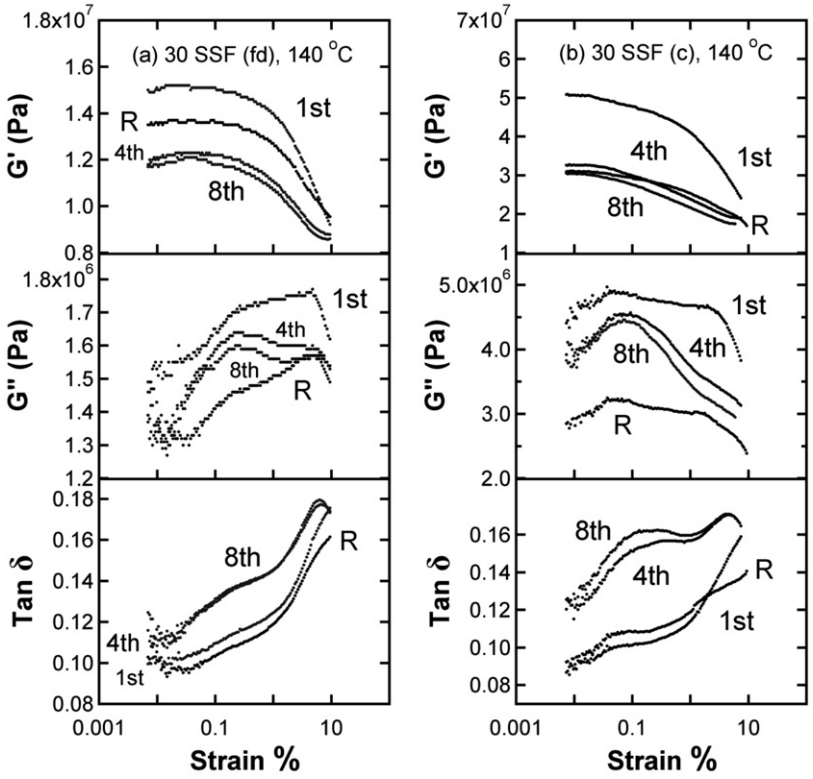

Fig. 5. Strain sweep experiments at 140 °C: (a) 30 wt% SSF composites prepared by freeze-drying method; (b) 30 wt% SSF composites prepared by casting method. Only 1st, 4th and 8th strain cycles are shown. *R* indicates the recovery curve after the samples are conditioned at 140 °C for 24 h.

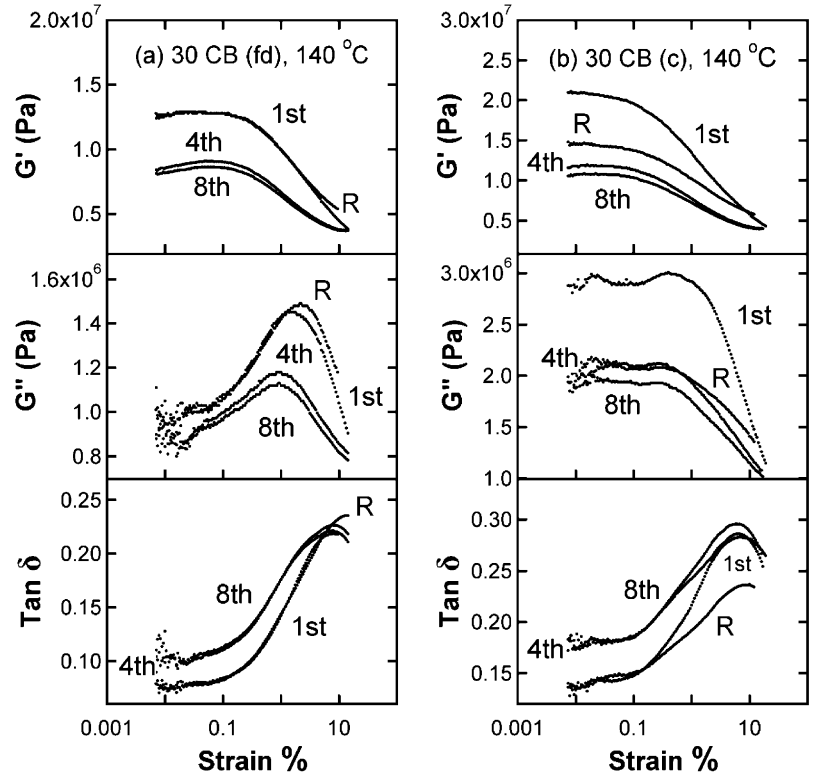

Fig. 6. Strain sweep experiments at 140 °C: (a) 30 wt% CB composites prepared by freeze-drying method; (b) 30 wt% CB composites prepared by casting method. Only 1st, 4th and 8th strain cycles are shown. *R* indicates the recovery curve after the samples are conditioned at 140 °C for 24 h.

CB composite prepared by the casting method has a G'' maximum at a smaller strain. These observations, again, indicate filler network structure produced by freeze-drying method is more elastic and less brittle than that by casting method.

3.4. Thermal mechanical properties of co-filler composites

Fig. 7 shows G' of co-filler composites with three different co-filler ratios. The general features of G' over the entire temperature range for the three different co-filler ratios are similar, but the G' decay in the glass transition region shows more than one transition in the insets of Fig. 7. The additional transitions can also be observed in Fig. 8, where additional G'' transitions occur at a higher temperature than that of the loss maximums in Fig. 3.

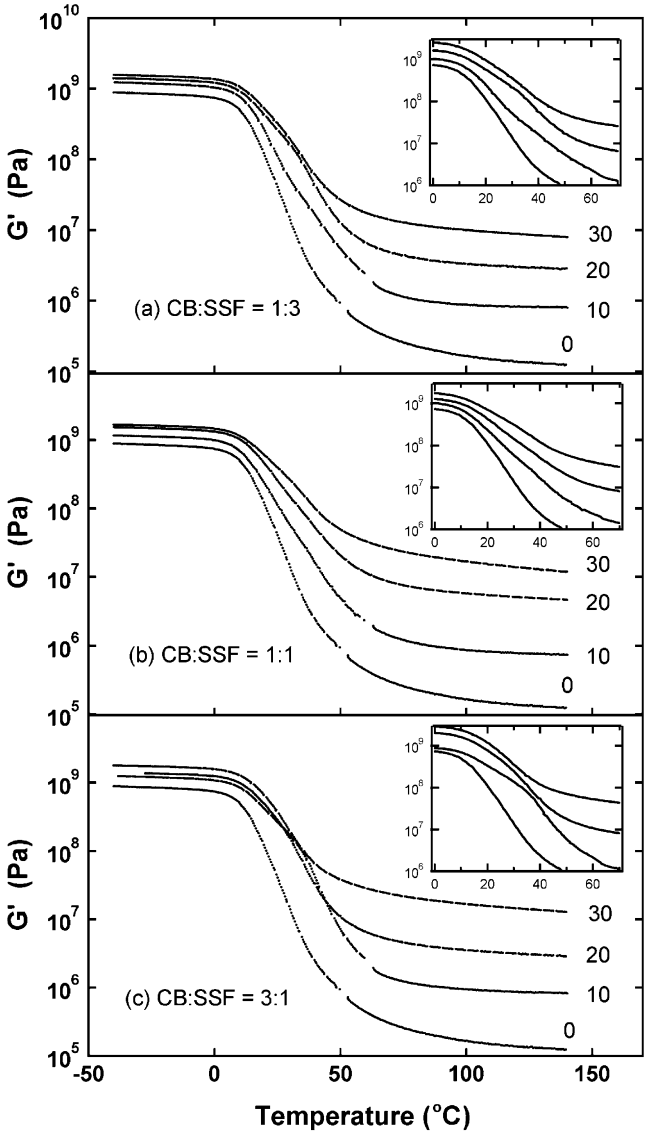

Fig. 7. Elastic moduli of co-filler composites. The weight fraction of co-filler is indicated at the end of each curve. The co-filler ratios are indicated in the graphs.

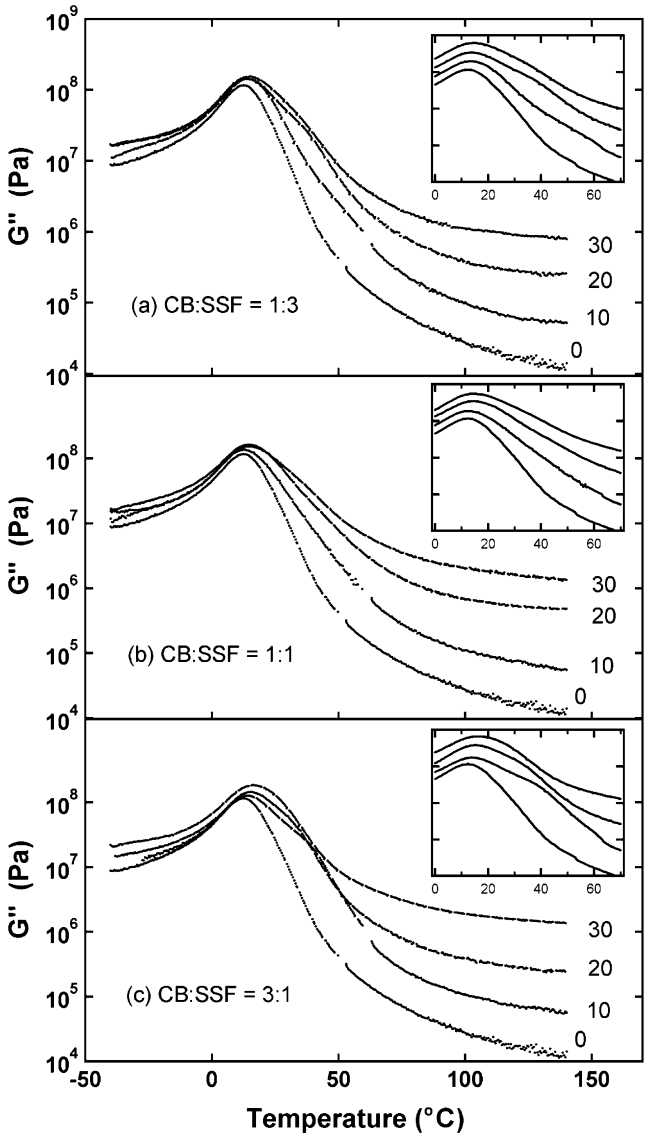

Fig. 8. Loss moduli of co-filler composites. The weight fraction of co-filler is indicated at the end of each curve. The co-filler ratios are indicated in the graphs.

These additional transitions are more easily observed on the 10% and 20% filled composites, and at the co-filler ratios of 1:3 and 3:1. These additional transitions become more obvious in the tan δ plots (Fig. 9), where two transitions are clearly observed for almost all compositions. The higher temperature tan δ transitions are listed in Table 1. It is obvious that the higher temperature tan δ transitions cannot be assigned to either the effect of CB or SSF. The higher temperature transitions in the glass transition region are attributed to the co-filler effect because neither the SSF or CB composites show such double transitions in Fig. 4. Since the rubber and fillers of co-filler composites are the same as that in the SSF or CB composites, the additional higher temperature transitions can only be attributed to the presence of regions of highly immobilized polymer chains between filler aggregates. These highly immobilized

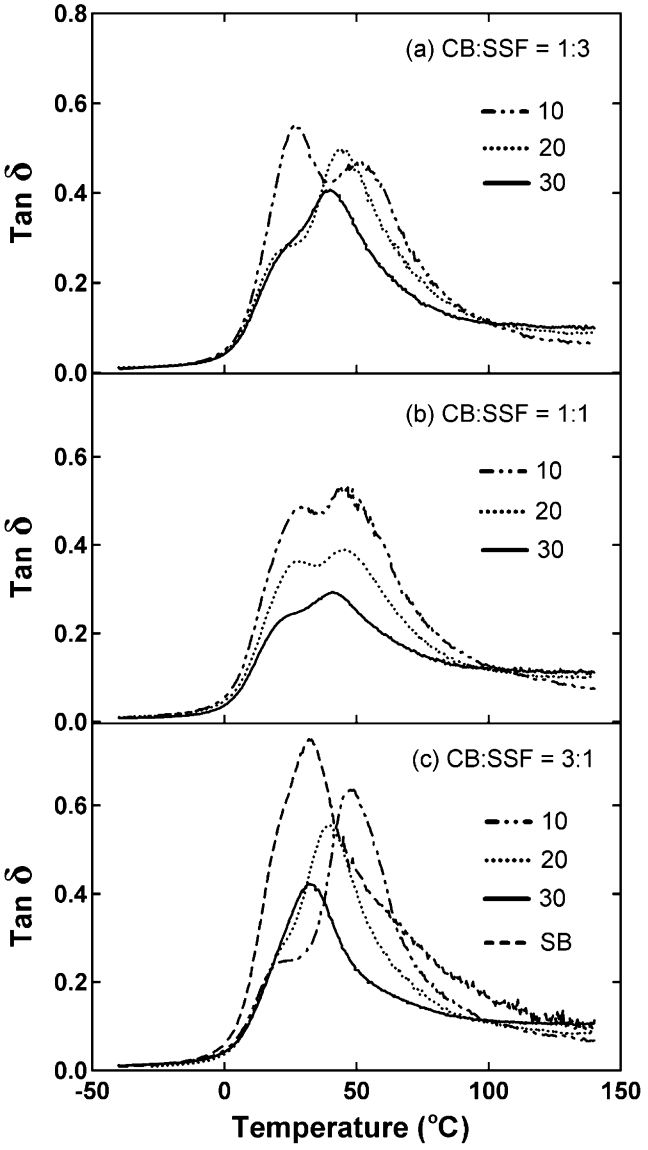

Fig. 9. Loss tangent of co-filler composites. The weight fraction of co-filler is indicated at the end of each curve. The co-filler ratios are indicated in the graphs.

Table 1
tan δ Maximums[a]

Composition	10% filler (°C)	20% filler (°C)	30% filler (°C)
SSF	25.6	25.0	24.6
CB	32.4	28.5	25.4
SPI	21.5	19.5	17.0
Co-filler			
CB:SSF = 1:3	50.9	45.6	40.0
CB:SSF = 1:1	45.4	45.4	41.6
CB:SSF = 3:1	48.9	40.0	31.9
CB:SPI = 1:1		32.6	

[a] Only higher temperature transitions for the co-filler composites are listed. tan δ Maximum for SB matrix is 31.9 °C.

polymer chains do not occur between SSF and SSF aggregates or CB and CB aggregates because it lacks a corresponding higher temperature transition over the same concentration range (Fig. 4). Filler–rubber interactions are also not the reason for such double transitions because same fillers are used in these composites. These observations indicate the regions of highly immobilized polymer chains are caused by a higher degree of confinement from the combination of SSF and CB filler aggregates.

Since SSF contains a small fraction of soy protein along with soy carbohydrate, it is desirable to determine if soy protein contributes to the regions of highly immobilized polymer chains. The effect of soy protein in SSF can be measured by combining the soy protein and carbon black as co-filler. The result is shown in Fig. 10, where a 20% co-filler reinforced composite containing 1:1 ratio of soy protein and CB shows only one loss tangent maximum at 32.6 °C (Table 1). On the other hand, the SSF co-filler composites with the same filler ratio have two tan δ maximums. The higher temperature transition occurs at 45.4 °C (Fig. 9(b) and Table 1). The absence of a higher temperature tan δ maximum in the SPI:CB composite indicate SPI in the SSF:CB co-filler composites does not contribute to the formation of regions of highly immobilized polymer chains.

For practical purposes, the G' of all co-filler reinforced composites are summarized in Fig. 11. Comparing with CB composites prepared by the same freeze-drying method, all co-filler composites show a greater elastic modulus in the rubber plateau region especially at 10% and 20% filler concentration. At 30% filler concentration, all compositions show a similar G'. This indicates the substitution of CB with more economical SSF leads to an increase in the elastic modulus of the composite, but with reduced filler cost. Comparing with SSF composites, the co-filler reinforced composites have a similar elastic modulus, but they have a better recovery behavior as will be shown in their stress softening effect.

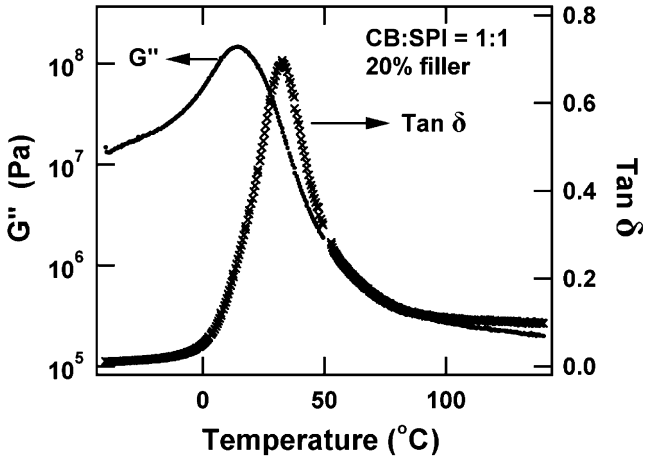

Fig. 10. Loss modulus and loss tangent of CB/SPI co-filler composites. The weight fraction of co-filler is 20%. Co-filler ratio CB:SPI = 1:1.

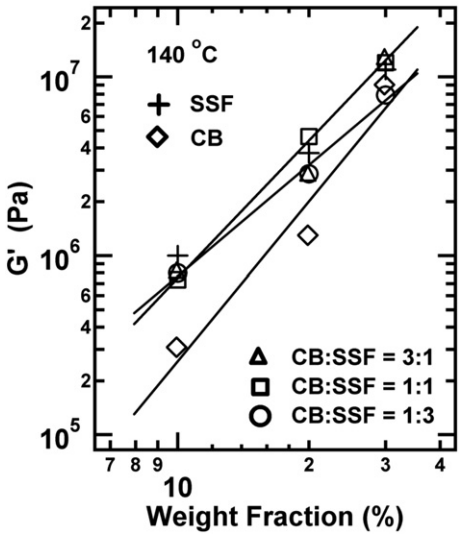

Fig. 11. Elastic moduli of co-filler composites at 140 °C. The SSF and CB composites are also included for comparison.

3.5. Stress softening effect of co-filler composites

The stress softening effect of co-filler composites is shown in Fig. 12. The retention of G' in the small strain region can be used to evaluate the instant recovery behavior after the eight cycles of strain deformation. Thus, the G' at 0.05% strain in the eighth cycle of the composites shown in Fig. 12(a), (b), and (c) retains 79%, 78%, and 74% G' of their first cycles, respectively. Comparing with the retention of ~80% G' (Fig. 5(a)) for the SSF composite and ~67% G' (Fig. 6(a)) for the CB composite, co-filler reinforced composites show more G' retention than the CB composites. All the co-filler composites with 30% filler content also show a total recovery of G' after the deformed composites were reconditioned at 140 °C for 24 h. For loss modulus under consecutive strain cycles, the energy dissipation process of co-filler composites became less pronounced and the maximum was shifted to the smaller strain amplitudes. The structure responsible for the energy dissipation process is obviously reduced after the first three cycles. After the major structure is broken down in the first three strain cycles, the remaining structure in the fourth and eighth strain cycles generates a broader loss maximum. The loss maximums in their first cycles occurred at 2.5%, 1.6%, and 1.6% for the composite in Fig. 12(a), (b), and (c), respectively. A loss maximum of a composite that occurs at a higher % strain indicates a more elastic structure, which requires a greater extent of deformation to break down the filler related structure. It is also noted that G' maximums occur in the small strain region in Fig. 12. These G' maximums are similar to the previous observation on the soy protein filled rubber composites and are attributed to the breaking down of filler-immobilized polymer networks [31]. Fig. 13 shows the strain dependent behavior of SB rubber matrix prepared by freeze-drying method at the glass transition temperature (10 °C) and at a temperature (25 °C) above the glass transition temperature. It is noted that the magnitude of both G' and G'' maximums is reduced and the peak width is broadened as temperature

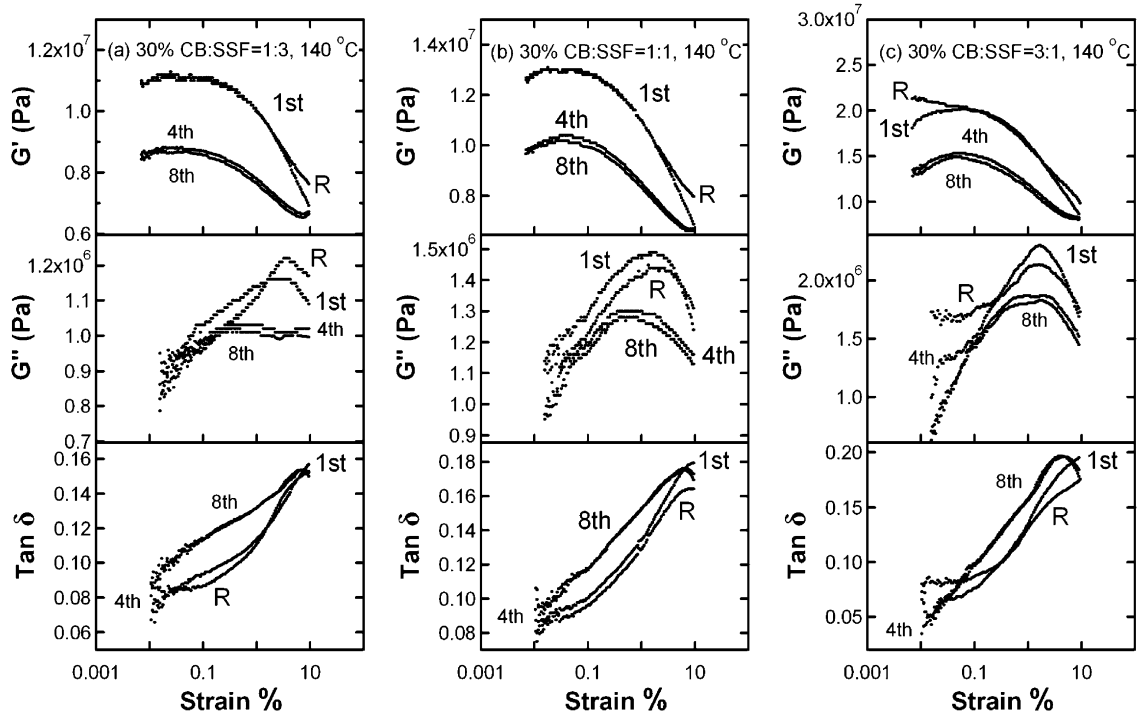

Fig. 12. Strain sweep experiments of composites reinforced by 30 wt% co-filler at 140 °C. Co-filler ratios are indicated in the graphs. Only 1st, 4th and 8th strain cycles are shown. *R* indicates the recovery curve after the samples are conditioned at 140 °C for 24 h.

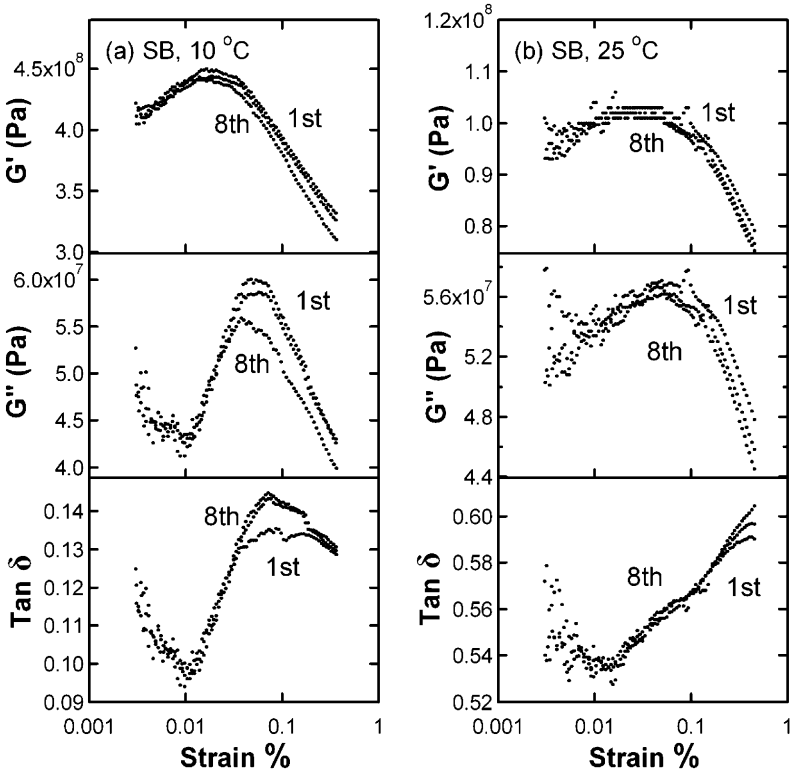

Fig. 13. Strain sweep experiments of SB rubber prepared by freeze-drying method: (a) experiments conducted at 10 °C; (b) experiments conducted at 25 °C. Only 1st, 4th and 8th strain cycles are shown.

increases. The increasing temperature reduces the amount of structure responsible for G'' maximum (Fig. 13(a)) and therefore reduces the magnitude of G'' maximum (Fig. 13(b)). The G' maximum of immobilized SB matrix occurred at 0.02–0.03% strain and is similar to the G' maximums in the co-filler composites that occurred at 0.02–0.05% strain. The G' maximum of compressed molded SSF is at ~0.01% strain. This indicates low temperature immobilized polymer structure is mainly responsible for the G' maximums observed in the strain dependent behavior of the co-filler composites.

Another interesting observation is the recovery behavior of the composites with 20% filler (Fig. 14). The recovery curves in these three composites all lie above the G' of the first strain cycle. This indicates the composite structure was changed by the eight consecutive deformation cycles and rearranged to form a stronger structure upon reconditioning at 140 °C for 24 h. One possible explanation is that the composite structure prepared by freeze-drying method was frozen in a homogeneous state, which was not an equilibrium state compared with that by casting method that allows a much longer time for a filler network to form. At 20% filler level, the composite is still soft enough for the structure to rearrange itself after the perturbation by the deformation cycles and to reach a more equilibrium state. To further analyze the major contribution of this behavior, the strain dependent behaviors of the composites with 20% SSF or CB filler were measured and shown in Fig. 15. Fig. 15(a) shows that the recovery curve of the SSF composite did not exceed the G' of the first cycle, but Fig. 15(b) shows that the recovery curve of the CB composite exceeds the G' of the first cycle. This is an indication that CB is responsible for the structure rearrangement in the co-filler composites. The mechanism of such rearrangement is not known, but possibly due to ability of smaller CB aggregates to diffuse in a softer rubber matrix to form a more connected filler related network.

For the loss tangent properties, the magnitude of tan δ for the co-filler composites is similar to that of the CB composites. The magnitude of tan δ has practical importance in rubber applications such as tire application. A rubber composite that has a smaller tan δ value tends to have a reduced rolling resistance and save energy, while a larger tan δ tends to have an improved skid resistance and wet grip. The ability of SSF to absorb some moisture in a wet state tends to reduce G' and increase tan δ and lead to a better wet traction.

3.6. Reversible strain dependence of shear elastic modulus

The reduction of shear elastic modulus with increasing strain is a familiar phenomenon reported by Payne [32–34] on carbon black filled rubbers in the early 1960s. Later Kraus [35] proposed a phenomenological model based on Payne's postulation of filler networking. The model is based on the aggregation and de-aggregation of carbon black agglomerates. In this model, the carbon black

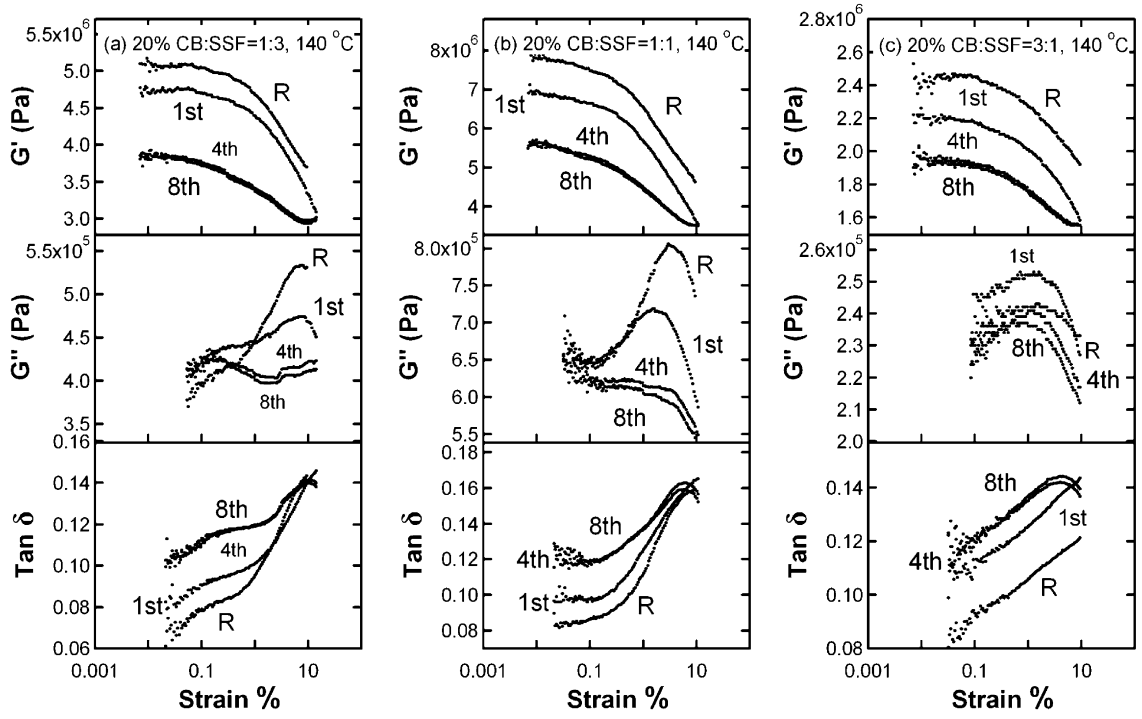

Fig. 14. Strain sweep experiments of composites reinforced by 20 wt% co-filler at 140 °C. Co-filler ratios are indicated in the graphs. Only 1st, 4th and 8th strain cycles are shown. *R* indicates the recovery curve after the samples are conditioned at 140 °C for 24 h.

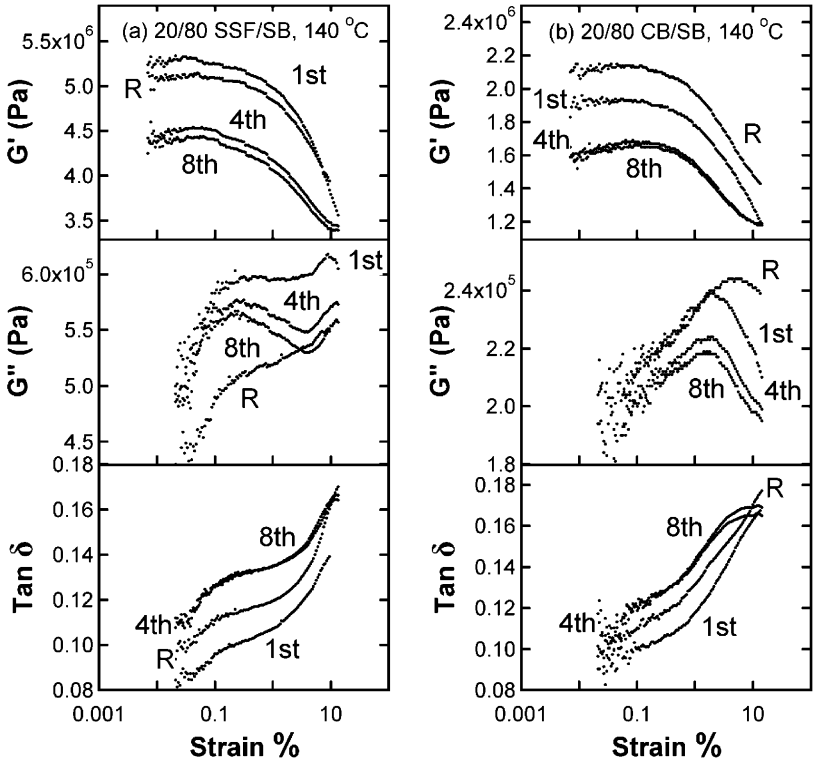

Fig. 15. Strain sweep experiments of composites reinforced by 20 wt% filler prepared by freeze-drying method: (a) SSF composite; (b) CB composite. Only 1st, 4th and 8th strain cycles are shown. *R* indicates the recovery curve after the samples are conditioned at 140 °C for 24 h.

contacts are continuously broken and reformed under a periodic sinusoidal strain. Based on this kinetic aggregate forming and breaking mechanism at equilibrium, elastic modulus was expressed as follows:

$$\frac{G'(\gamma)-G'_{\infty}}{G'_0-G'_{\infty}}=\frac{1}{1+(\gamma/\gamma_c)^{2m}} \quad (1)$$

where G'_{∞} is equal to $G'(\gamma)$ at very large strain, G'_0 is equal to $G'(\gamma)$ at very small strain, γ_c is a characteristic strain, where $G'_0-G'_{\infty}$ is reduced to half of its zero-strain value, and m is a fitting parameter related to filler aggregate structures. Eq. (1) has been shown to describe the behavior of $G'(\gamma)$ in carbon black filled rubber reasonably [15]. The loss modulus and loss tangent, however, do not have a good agreement with experiments [36], mainly because of the uncertainty in the formulation of loss mechanism. In this study, an empirical fit is useful to show the difference in their strain behaviors (Fig. 16 and Table 2) between the different composites. In general, a smaller fitting parameter m indicates a more rapid and continuous decrease of G' with increasing strain and suggests a more rapid and continuous breaking up of filler network structure as the strain is increased. On the other hand, a larger m indicates a more elastic structure, which breaks down at a lower rate and has a plateau-like modulus in the small strain region. From

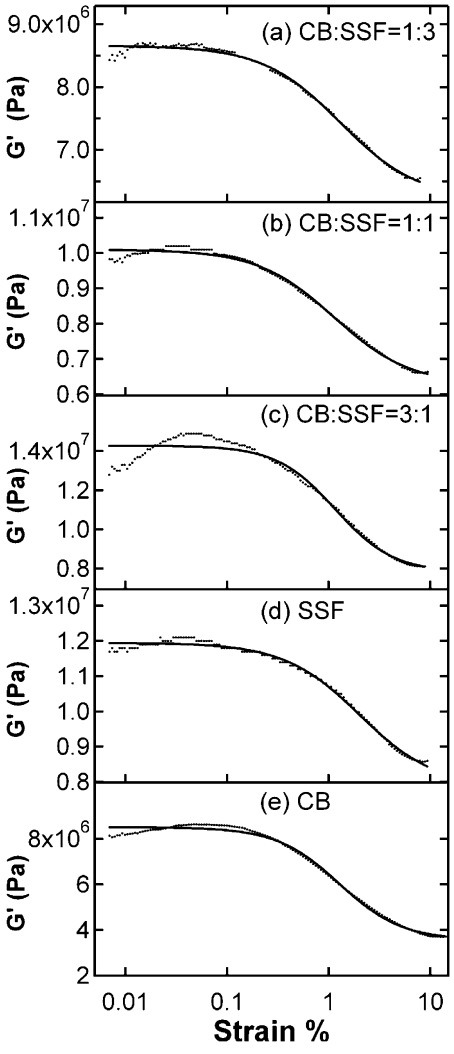

Fig. 16. The 8th cycle of strain sweep experiments at 140 °C and 1 Hz. Solid lines are the fit from the Kraus model.

Table 2
Fit parameters of shear elastic modulus[a]

Composition	Best fit[b] m	γ_c(%)	G'_0(MPa)	G'_{∞}(MPa)
Freeze-dry				
SSF (fd)	0.58 ± 0.06	2.02 ± 0.07	11.9 ± 0.05	7.85 ± 0.33
CB (fd)	0.71 ± 0.07	1.27 ± 0.11	8.51 ± 0.07	3.56 ± 0.19
Co-filler (freeze-dry)				
CB:SSF = 1:3	0.57 ± 0.06	1.30 ± 0.17	8.66 ± 0.03	6.21 ± 0.15
CB:SSF = 1:1	0.58 ± 0.06	1.12 ± 0.14	10.1 ± 0.06	6.28 ± 0.21
CB:SSF = 3:1	0.76 ± 0.19	1.16 ± 0.25	14.3 ± 0.21	7.81 ± 0.69
Casting				
SSF (c)	0.34 ± 0.02	0.67 ± 0.06	31.6 ± 0.19	13.8 ± 0.56
CB (c)	0.49 ± 0.02	1.00 ± 0.05	11.0 ± 0.06	3.45 ± 0.14

[a] All are 30% filled composites. The data are from the 8th strain cycle measured at 140 °C.
[b] Best fit of shear elastic modulus vs. strain with the Kraus Model.

Fig. 16 and Table 2, the fitting using the Kraus model is generally acceptable except when a filler is dominated by CB, where a G' maximum in the small strain region prevents a good fit. Comparing m values in Table 2 between freeze-drying and casting samples, the value of m is generally larger for the composites prepared by freeze-drying method and indicates a more elastic structure, consistent with polymer mediated filler network structure discussed previously. Also, the m values of the co-filler composites indicate the strain dependent behavior of the co-filler composites is similar to that of the SSF or CB filled composites prepared by the freeze-drying method.

4. Conclusions

SSF, CB, and the mixtures of SSF and CB are used as fillers to make reinforced rubber composites by blending the dispersions of filler and rubber latex in aqueous phase and followed by freeze-drying and compression molding. 10%, 20% and 30% filled composites are studied and compared in terms of their viscoelastic properties. Comparison between freeze-drying and casting method indicates filler network related structure in the composites prepared by freeze-drying method is more elastic than that by casting method and can be explained by the model of polymer mediated filler network. The shifting of G'' maximum in SSF and CB composites with increasing filler concentration indicates CB has a greater extent of filler–rubber interaction. The stress softening effect of SSF and CB composites again indicates the composites prepared by freeze-drying method have better recovery behavior than that by casting method due to their more elastic filler network structure. Thermal mechanical measurements of co-filler composites revealed two glass transitions with one transition occurred at a higher temperature caused by the effect of co-filler. The co-filler composites were also studied with the dynamic strain sweep experiments to understand the filler related structures. All the 30% co-filler composites show a 100% modulus recovery compared with a 90% recovery in the 30% SSF composite, indicating the co-filler network

structure is more elastic. G' maximums in the strain sweep experiments are attributed to the deformation of filler-immobilized polymer network. That the modulus of recovery in the 20% co-filler composites exceeds the G' of the first strain cycle is attributed to the rearrangement of non-equilibrated filler network structure to form a stronger and more equilibrated structure. The reversible modulus–strain curves of SSF, CB, and co-filler composites at 140 °C were empirically fitted with the Kraus model. The fitting parameter m for co-filler composites was found to be similar to that of SSF or CB composites prepared by the same method. This suggests the elasticity of co-filler network structure is similar to that of CB composites. This study shows the use of SSF to partially substitute CB as the reinforcement co-filler produces rubber composites with favorable viscoelastic properties and economic value.

Acknowledgements

The author thanks various industrial companies for supplying materials used in this study and A.J. Thomas for the calibration and maintenance of rheological instruments.

References

[1] Ismail H, Jaffri RM, Rozman HD. The effects of filler loading and vulcanization system on properties of oil palm wood flour-natural rubber composites. J Elastomers Plast 2003;35(2):181–92.
[2] Nair KG, Dufresne A. Crab shell chitin whisker reinforced natural rubber nanocomposites. 2. Mechanical behavior. Biomacromolecules 2003;4:666–74.
[3] Ismail H, Shuhelmy S, Edyham MR. The effect of a silane coupling agent on curing characteristics and mechanical properties of bamboo fiber filled natural rubber composites. Eur Polym J 2001;38(1):39–47.
[4] Wang C, Carriere CJ. Blends of biodegradable poly(hydroxy ester ether) thermoplastic with renewable proteins. US Patent 6 310 136 B1; 2001.
[5] Wang S, Sue HJ, Jane J. Effects of polyhydric alcohols on the mechanical properties of soy protein plastics. J M S – Pure Appl Chem 1996;A33(5):557–69.
[6] Paetau L, Chen C, Jane J. Biodegradable plastic made from soybean products. 1. Effect of preparation and processing on mechanical properties and water absorption. Ind Eng Chem Res 1994;33:1821–7.
[7] Mo X, Sun XS, Wang Y. Effects of Molding temperature and pressure on properties of soy protein polymers. J Appl Polym Sci 1999;73:2595–602.
[8] Wu Q, Zhand L. Properties and structure of soy protein isolate-ethylene glycol sheets obtained by compression molding. Ind Eng Chem Res 2001;40:1879–83.
[9] Coughlin ETA. Floor covering. US Patent 2 056 958; 1936.
[10] Isaacs MR. Composition of matter. US Patent 2 127 298; 1938.
[11] Lehmann RL, Petusseau BJ, Pinazzi CP. Preparation of rubber–protein–glyoxal composition and vulcanizable material obtained therefrom. US Patent 2 931 845; 1960.
[12] Fuetterer CT. Anti-skid tire treads and rubber stock therefor. US Patent 3 113 605; 1963.
[13] Beckmann O, Teves R, Loreth W. Rubber compounds for treads for winter tires. Ger Offen DE 19622169 A1 19961212; 1996.
[14] C. Recker. With sulfur vulcanizable rubber compositions containing proteins from oilseeds for winter tire treads. Eur Pat Appl EP 1234852 A1 20020828; 2002.
[15] Heinrich G, Kluppel M. Recent advances in the theory of filler networking in elastomers. Adv Polym Sci 2002;160:1–44.
[16] Wang MJ. Effect of polymer–filler and filler–filler interactions on dynamic properties of filled vulcanizates. Rubber Chem Technol 1998;71:520–89.
[17] Richard J. Dynamic micromechanical properties of styrene–butadiene copolymer latex films. Polymer 1992;33(3):562–71.
[18] Zosel A, Ley G. Influence of cross-linking on structure, mechanical properties, and strength of latex films. Macromolecules 1993;26:2222–7.
[19] Kan CS, Blackson JH. Effect of ionomeric behavior on the viscoelastic properties and morphology of carboxylated latex films. Macromolecules 1996;29:6853–64.
[20] Garcia MC, Torre M, Marina ML, Laborda F. Composition and characterization of soybean and related products. Crit Rev Food Sci Nutr 1997;37(4):361–91.
[21] Jong L. Rubber composites reinforced by soy spent flakes. Polym Int 2005;54(11):1572–80.
[22] Carter CM, Cravens WW, Horan FE, Lewis CJ, Mattil KF, Williams LD. Oilseed proteins. In: Milnre M, Scrimshaw NS, Wang DIC, editors. Protein resources and technology. Connecticut: AVI Publishing; 1978. p. 282–4.
[23] Chazeau L, Brown JD, Yanyo LC, Sternstein SS. Modulus recovery kinetics and other insights into the Payne effect for filled elastomers. Polym Compos 2000;21(2):202–22.
[24] Jong L. Dynamic mechanical properties of soy protein filled elastomers. J Polym Environ 2005;13(4):329–38.
[25] Yurekli K, Krishnamoorti R, Tse MF, Mcelrath KO, Tsou AH, Wang HC. Structure and dynamics of carbon black-filled elastomers. J Polym Sci: Part B: Polym Phys 2001;39:256–75.
[26] Vieweg S, Unger R, Hempel E, Donth E. Kinetic structure of glass transition in polymer interfaces between filler and SBR matrix. J Non-Crystalline Solids 1998;235/237:470–5.
[27] Jong L. Characterization of soy protein/styrene–butadiene rubber composites. Compos: Part A 2005;36:675–82.
[28] Mele P, Marceau S, Brown D, Puydt Y, Alberola D. Reinforcement effects in fractal-structure-filled rubber. Polymer 2002;43:5577–86.
[29] Mullins L. Effect of stretching on the properties of rubber. J Rubber Res 1947;16:275–89.
[30] Mullins L. Thixotropic behavior of carbon black in rubber. Phys Colloid Chem 1950;54:239–51.
[31] Jong L. Viscoelastic properties of ionic polymer composites reinforced by soy protein isolate. J Polym Sci: Part B: Polym Phys 2005;43(24):3503–18.
[32] Payne AR. The dynamic properties of carbon black-loaded natural rubber vulcanizates. Part I. J Appl Polym Sci 1962;6(19):57–63.
[33] Payne AR. The dynamic properties of carbon black-loaded natural rubber vulcanizates. Part II. J Appl Polym Sci 1962;6(21):368–72.
[34] Payne AR. Dynamic properties of heat-treated butyl vulcanizates. J Appl Polym Sci 1963;7:873–85.
[35] Kraus G. Mechanical losses in carbon-black-filled rubbers. J Appl Polym Sci, Appl Polym Symp 1984;39:75–9236.
[36] Ulmer JD. Strain dependence of dynamic mechanical properties of carbon black-filled rubber compounds. Rubber Chem Technol 1995;69:15–47.